

## A Novel Four-Element Button Mushroom MIMO Antenna for Enhanced Sub-6 GHz 5G Communication

Kakade Sandeep<sup>1\*</sup>, Deshpande Asmita<sup>1</sup>, Patil Shrishail<sup>2</sup>, Nitin Shivale<sup>2</sup>, Vijay Sonawane<sup>2</sup>

<sup>1</sup>Vilasrao Deshmukh Foundation Group of Institutions, Latur, India, <sup>2</sup>Bhivarabai Sawant Institute of Technology and Research, Pune, India. \*Corresponding Author's Email: kakadesandeep2000@gmail.com

### Abstract

This paper presents a high-performance four-element button mushroom MIMO antenna tailored for sub-6 GHz fifth-generation (5G) wireless communication systems. The antenna is fabricated on an FR4 epoxy substrate with a dielectric constant of 4.4 and a thickness of 1.6 mm, offering a cost-effective and mechanically robust solution. The design comprises rectangular patch elements optimized for dual-band operation at 3.48 GHz and 4.75 GHz, effectively covering key segments of the sub-6 GHz 5G spectrums. A button mushroom structure is incorporated between elements to significantly reduce mutual coupling and enhance isolation, achieving values consistently below -20 dB across the targeted bands. Simulations conducted using Ansys HFSS demonstrated excellent MIMO performance, with an envelope correlation coefficient (ECC) of less than 0.03, channel capacity loss (CCL) below 0.4 bits/s/Hz, and diversity gain (DG) approaching 10 dB. The antenna supports a total bandwidth of 2.11 GHz, ensuring reliable wideband performance. Experimental validation using a vector network analyzer and anechoic chamber confirmed the simulation outcomes. The compact size, high isolation, and wide operational bandwidth make the proposed antenna a strong candidate for modern 5G MIMO applications. Future enhancements may include the integration of tunable components for dynamic frequency adaptability and Specific Absorption Rate (SAR) analysis for user safety and regulatory compliance.

**Keywords:** C-band, Multiple Input Multiple Outputs, n77, n78, 5G Application.

### Introduction

The swift development of wireless communication, particularly the fifth-generation (5G) technology, has spurred the need for high-performance antennas that can support faster data rates, wider bandwidth, and higher spectral efficiency. The sub-6 GHz spectrum is a critical component of 5G technology due to its ability to offer a balance between coverage and capacity. MIMO antennas have become important facilitators in this regard, enabling better communication through multiplexing over space, higher data throughput, and greater network dependability. MIMO antenna design for 5G applications offers several challenges, including maintaining compact size, achieving wide bandwidth, and ensuring high isolation between antenna elements. Metasurface-based designs have shown promise in addressing these challenges (1). A small, wideband, and highly isolated MIMO antenna was created for 5G applications, highlighting the significance of improving antenna performance and reducing mutual coupling. MIMO antennas with superior

isolation have been proposed to meet the requirements of 5G New Radio (NR) applications, which further highlight the need for efficient designs in limited form factors (2, 3). The challenges of compactness, high isolation, and enhanced bandwidth in MIMO systems have been addressed by various design approaches. This has brought attention to the importance of optimizing MIMO antenna structures for a range of applications by utilizing creative design strategies that improve isolation and boost performance across multiple frequency bands. Their analysis demonstrated the growing popularity of antenna design techniques such as slot antennas, dielectric resonators, and metamaterials. All of these contribute to increased diversity and reduced coupling in MIMO systems (4). Mutual coupling between components of a MIMO antenna poses a major challenge, as it can degrade system performance by increasing interference and reducing overall efficiency. One of the most effective approaches for addressing mutual

This is an Open Access article distributed under the terms of the Creative Commons Attribution CC BY license (<http://creativecommons.org/licenses/by/4.0/>), which permits unrestricted reuse, distribution, and reproduction in any medium, provided the original work is properly cited.

(Received 2<sup>nd</sup> November 2024; Accepted 10<sup>th</sup> April 2025; Published 30<sup>th</sup> April 2025)

coupling is the application of defected ground structures (DGS). DGS involves introducing deliberate disruptions in the ground plane of the antenna, which can modify current distribution and suppress unwanted coupling between antenna elements. How a DGS-based design can significantly reduce mutual coupling in a two-port MIMO antenna, leading to better isolation and enhanced performance for 5G systems. The research highlights the effectiveness of DGS in minimizing the negative impact of closely spaced antennas, especially in compact configurations required for modern wireless devices (5). MIMO systems use a variety of antenna elements to boost signal reliability and data throughput. Conversely, mutual coupling may lead to poorer performance, less channel capacity, and a decline in diversity gain (DG). Thus, ensuring optimal system performance, especially in compact designs, requires achieving sufficient isolation between antenna components (6). The paper builds on recent advances in MIMO antenna design and proposes a novel button mushroom slotted patch MIMO antenna that deals with the problem of reciprocal coupling while staying small. By achieving high isolation and maintaining efficient radiation characteristics, the suggested antenna design is suitable for implementation in 5G devices and base stations operating in the Sub-6 GHz spectrum. In summary, MIMO antenna systems play a crucial role in advancing 5G technology by enhancing data rates, signal quality, and overall network capacity. By using multiple antennas to reduce interference and increase spectral efficiency, these designs are pivotal in meeting the demands of high-speed and high-capacity wireless communications essential for modern applications like IoT, smart cities, and immersive media experiences. In recent years, MIMO antenna systems have been extensively researched to develop compact, high-performance designs suitable for 5G and other advanced applications. In order to support larger data rates and enhance signal quality in dense user situations, these designs usually concentrate on improving factors like isolation, bandwidth, and gain. Methods including employing electromagnetic band gap (EBG) and DGS, utilizing decoupling structures, and adding parasitic elements have demonstrated encouraging outcomes in lowering mutual coupling and increasing efficiency. They show how

using dielectric resonator antennas (DRAs) in four-port MIMO systems can improve bandwidth and isolation by taking advantage of high permittivity materials that reduce cross-port interference. These developments make it possible to incorporate small MIMO systems that meet the demanding performance standards of contemporary wireless networks. This study investigates a high-isolation MIMO antenna design optimized for 5G C-band applications by employing a combination of DRA, EBG, and DGS techniques. The objective is to improve the effectiveness of massive antennas, crucial for the 5G network, where high isolation between antenna elements mitigates mutual coupling effects that degrade signal quality. The proposed design utilizes an  $8 \times 8$  array configuration at 3.5 GHz, with an FR-4 substrate and DRA-EBG-DGS implementation, achieving a significant increase in gain (24.7 dB), bandwidth (246 MHz), and a reduction in envelope correlation coefficient (ECC), highlighting improved isolation and overall antenna efficiency (7). Significantly lowering mutual coupling between parts to less than -32 dB, the antenna system uses a new decoupling structure and operates at 28 GHz. DGS, frequency-selective surfaces, metamaterials, and decoupling structures are some of the methods that have been commonly employed to improve MIMO antenna element separation. To improve mutual connection, for instance, metastructures have been employed; nonetheless, they frequently call for intricate and sizable geometries. Parasitic patches, which have been successfully used to minimize coupling while preserving compactness, may still encounter difficulties due to their limited bandwidth. This study's decoupling structure streamlines the antenna design, allowing for a small  $10 \text{ mm} \times 10 \text{ mm}$  footprint while preserving strong isolation and broad bandwidth (8). The importance of antenna design in 5G communication systems is covered in this article, with particular attention paid to the utilization of higher frequency bands such as millimeter wave. For antennas, a substrate thickness of 0.127 to 0.787 mm is ideal; thinner substrates are favored. Antenna arrays and their application to increase reflection coefficients are also covered in the essay. The study comes to the conclusion that in order for 5G networks to support increased data rates and the internet of things (IoT), appropriately

constructed antennas are essential (9). A MIMO antenna with two symmetrical hexagon-shaped radiators and an inverted T-shaped ground structure is studied using the CST simulator. Features that are the primary focus of the inquiry include radiation patterns, effective gain, S-parameters, and current distribution. The antenna exhibits a strong correlation between the simulated and measured data, with an efficiency of 88% and a gain of over 4.5 dB (10). For medical applications, ISM networks are designed to be utilized with a printed planar 4-element MIMO antenna. Featuring four ground planes and dragonfly-shaped radiators, it provides more than 21.4 dB isolation between 2.16 GHz and 3.2 GHz. The antenna is ideal for medical ISM applications due to its low ECC values, reliable radiation behavior, exceptional diversity performance, and small size. ISM systems in medical contexts seem to have a bright future because of their greater isolation between antenna ports (11). An enhanced isolation high-gain antenna employing FR-4, metasurface, and frequency-selective surface. It has an 8.44 dBi peak gain and less than 20 dB element isolation. It has a 96% maximum efficiency, a 92.3% correlation coefficient decrease, 9.99 DG, and 0.01 ECC (12). For a 5G MIMO system operating at 38 GHz, a compact, self-isolated slot antenna construction has been developed. The antenna matches the microstrip to the T-type folding substrate-integrated waveguide (SIW) feeding section impedance and reduces feed line near-field coupling. The highest gain is 10 dBi, while the lowest isolation is 30 dB, and the impedance bandwidth is 7.17%. The antenna shows promise for 38 GHz 5G MIMO applications due to its enhanced performance and compact design (13). A small, orthogonally polarized MIMO antenna array is presented in this study. It is intended for use in mmWave frequencies in next-generation 5G communication systems. The design aims to achieve high isolation, minimal envelope correlation, and consistent radiation efficiency throughout 26.2–34.2 GHz using diamond-shaped radiators and a corporate feed structure. According to the literature, the majority of 5G MIMO antenna systems use techniques like parasitic components and metamaterials in an effort to maximize bandwidth and isolation. These solutions, however, often get larger and more complex. In order to meet the spatial variety and

channel capacity needs of 5G, the suggested design maintains a small footprint (26 x 16 mm), high gain (up to 7 dBi), and radiation efficiency above 90% (14). This paper introduces an eight-element MIMO antenna system developed for use in 5G smartphone applications. Covering the n77 frequency band (3.2–4.2 GHz), the proposed antenna system incorporates T-slot and inverted C-slot stubs on a compact FR-4 substrate to achieve wideband performance and high efficiency. The authors address challenges of mutual coupling between closely placed antenna elements by introducing slots for improved isolation (up to 14.5 dB) and achieve an ECC below 0.025, which enhances diversity gain and channel capacity. Performance metrics such as radiation and total efficiency exceed 60%, and the extreme channel capacity reaches 40 bps/Hz. The paper also explores the antenna's performance in the presence of a human model to ensure safe specific absorption rate (SAR) levels, demonstrating that the SAR remains below the recommended safety limit. Compared to existing designs, this antenna achieves a balance of bandwidth, efficiency, isolation, and low ECC, making it well-suited for integration into next-generation 5G smartphones (15). In this study, a slotted, wideband, eight-element antenna for smartphones operating in the n77 frequency range is presented. The antennas on a PCB are positioned specifically to enhance signal reception. The system achieves wideband, characteristics, radiation, and total efficiency above 60% and high ECC, DG, and CC. Utilizing an FR4 substrate, the design achieves a peak gain of 4.8 dBi and a -6 dB bandwidth of 1.12 GHz (16). A paper introduces a MIMO antenna system designed for millimeter-wave, utilizing a SIW to feed rectangular DRA. The design, intended to operate in the 24.5–27.5 GHz and 33–37 GHz bands, arranges the DRA elements in a cross shape, providing polarization and spatial diversity with high isolation between elements, achieving over 22 dB and 17 dB in each band without additional isolation methods. It maintains an ECC below 0.15, reducing channel interference and ensuring robust MIMO performance. The study confirms that measured results align well with simulations, making this antenna configuration promising for 5G networks where compact, high-isolation designs are essential. This research contributes to ongoing advancements in 5G antenna technology

by showcasing the benefits of SIW-fed DRA structures in compact MIMO systems (17). The paper presents wearable, circularly polarized MIMO antennas for wireless ultra-wideband (UWB) systems. The antenna's exceptional specifications include a 5.2-7.1 GHz axial ratio bandwidth, a 3.6-13 GHz impedance bandwidth, and a low channel capacity loss (CCL). It has twin-sense circular polarization, good isolation, and an  $ECC < 0.02$  and  $DG > 9.96$  dB. It is wearable due to its small size and layers of material. The absorption rate of the antenna in various human body conditions is also investigated. Perfect for WiMAX C-band uplink/downlink, WLAN, and Bluetooth (18). Compact, dual-polarized, wideband antennas are used in MIMO applications. A wideband hybrid ring coupler, cross magnetic dipoles, and parasitic resonators are employed. The antenna has a strong front-back ratio, low mutual coupling, and ECC. It is suitable for MIMO use despite its small size and high Q-factor-backed cavity restrictions (19). A small four-element antenna for 5G communications targeting the new radio n77 and n78 channels is shown in this study. Using HFSS software, the 40x40x1.6 mm antenna is designed and produced on FR-4. Protruded stubs and an "EH" slot enhance impedance matching and bandwidth. DG is close to 10 dB, and ECC is minimal, outperforming 5G antennas (20). The review as a whole shows significant progress in MIMO antenna design for a range of 5G applications, with a focus on compactness, isolation, and efficiency. Different antenna structures have been proposed by researchers for different bands. The selection of the button mushroom structure is driven by its compact design, improved radiation efficiency, and enhanced bandwidth, making it highly effective for sub-6 GHz 5G MIMO applications. Unlike conventional antenna geometries, it minimizes mutual coupling, improves isolation, and optimizes impedance matching, thereby ensuring superior multi-antenna performance. Additionally, its biomimetic structure enhances gain and stability, making it a suitable candidate for next-generation wireless networks. Advances in MIMO antenna technology will continue to be essential for future generations of wireless systems as the demand for faster data rates, better coverage, and more dependable communications grows. These developments are advancing MIMO antenna

technology and resolving compatibility, size, and isolation issues, improving 5G communication systems in a number of industries. The proposed button mushroom MIMO antenna is superior to conventional antenna designs for sub-6 GHz 5G applications due to its enhanced isolation, compact structure, and improved impedance matching. Traditional patch antennas often suffer from mutual coupling and limited bandwidth, whereas this design minimizes interference and supports stable radiation patterns. Additionally, its unique structure optimizes spatial diversity, ensuring reliable high-speed communication in dense 5G networks. These advantages make it a more effective solution compared to conventional approaches.

## Methodology

Due to its powerful electromagnetic simulation capabilities, which enable analysis and optimization of antenna performance in complex environments, we use the High-frequency structure simulator (HFSS). A comparative analysis of different substrate materials was conducted to evaluate their impact on the proposed MIMO antenna's performance. Factors such as dielectric constant, loss tangent, and overall efficiency were considered. FR4 was selected due to its cost-effectiveness, mechanical stability, and suitable dielectric properties. Compared to other high-performance substrates like Rogers and Teflon-based materials, FR4 offers a balance between affordability and acceptable electromagnetic properties. The chosen substrate provides optimal impedance matching, improved isolation, and enhanced bandwidth for sub-6 GHz 5G applications.

## Single Antenna Design

This MIMO antenna uses substrate FR4, which is 1.6 mm thick, and is built as a single antenna. The square patch design is frequently selected due to its ease of manufacture and simplicity. The square patch can function at a single frequency band depending on its size and is anticipated to have a broadside radiation pattern. The Maxwell equation is used to compute the geometrical designs of a simple antenna's patch, substrate, ground plane, and feed line. FR4, a material with a dielectric constant of 4.4 and a thickness of 1.5 mm, makes up the substrate's design. In the proposed work, the resonance frequency is 4.62 GHz. The many geometrical parameters of the patch antenna

design are assessed using these formulas. To find the patch's width, apply Equation 1.

$$W_p = \frac{c}{2f_r \sqrt{\frac{\epsilon_r + 1}{2}}} \quad \dots [1]$$

Here,  $W_p$  stands for the patch width,  $c$  for the speed of light, which is  $3 \times 10^8$  m/s,  $f_r$  for the resonance frequency, and  $\epsilon_r$  for the value of the dielectric constant. The patch's length can be found using,

$$L_p = L_{peff} - 2\Delta L_p \quad \dots [2]$$

In this case, the patch's effective length is indicated by  $L_{peff}$ , while its extension length is indicated by  $\Delta L_p$ , are derived by

$$L_{peff} = \frac{c}{2f_r \sqrt{\epsilon_{reff}}} \quad \dots [3]$$

$$\Delta L_p = 0.412h \frac{(\epsilon_{reff} + 0.3) \left(\frac{W_p}{h} + 0.264\right)}{(\epsilon_{reff} - 0.258) \left(\frac{W_p}{h} + 0.8\right)} \quad \dots [4]$$

Effective dielectric constant, represented by the symbol  $\epsilon_{reff}$ , is calculated by using the subsequent formula, where  $h$  stands for substrate thickness.

$$\epsilon_{reff} = \frac{\epsilon_r + 1}{2} + \frac{\epsilon_r - 1}{2} \left(1 + 12 \frac{h}{W_p}\right)^{-\frac{1}{2}} \quad \dots [5]$$

The following formula provides an approximation of the substrate's length and width.

$$L_s = 6h + L_p \quad \dots [6]$$

$$W_s = 6h + W_p \quad \dots [7]$$

#### Four-Element Antenna Array

The patch antenna is rectangular in shape, with a circular button mushroom structure on top and tiny slits at the base. There is a 1 mm thick microstrip feed line included. A C-shaped slit is built into the radiating element to lower surface current. The antenna is constructed on a 1.6 mm thick FR4 substrate. A modified ground with an arc-shaped construction and slots measuring 16 x 4.2 mm within each element makes up the 67.9 x 67.9 mm MIMO antenna. These adjustments are meant to boost the antenna's resonance at the target frequency while decreasing mutual coupling. The antenna system's radiation characteristics are improved by using an additional ground on the back of the radiating element. Each radiating element has an upturned L-shaped frame to increase isolation and MIMO performance. The disclosed antenna system's dual-antenna arrangement is intended to improve MIMO performance for 5G applications. Each of the four unique antenna elements in the design is symmetrically oriented around a central axis; the characteristics are displayed in Figure 1.

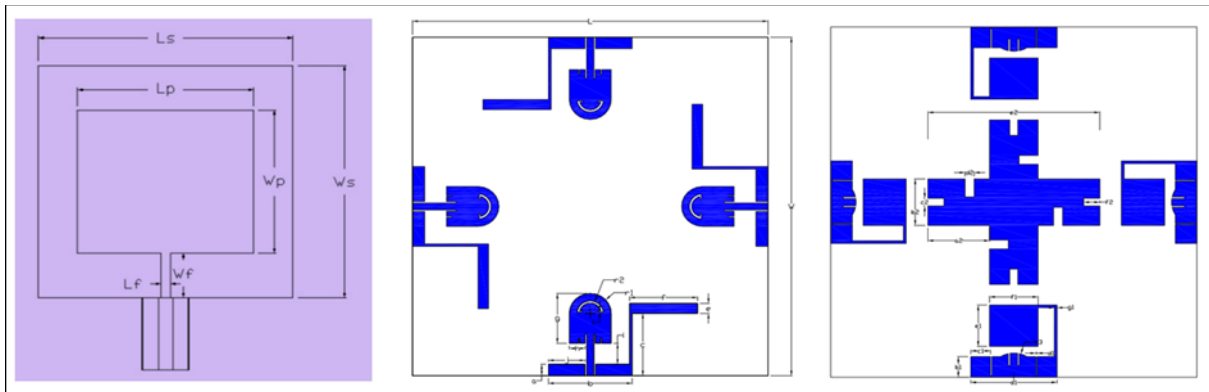


**Figure 1:** Geometry of (A) Rectangular Patch (B) MIMO Antenna Top View (C) Bottom View

#### MIMO Antenna Geometry

The proposed four-element button mushroom MIMO antenna, as depicted in figure 1, features a compact and precisely structured geometry designed for enhanced sub-6 GHz 5G communication. The optimized dimensions and inter-element spacing, detailed in table 1, improve

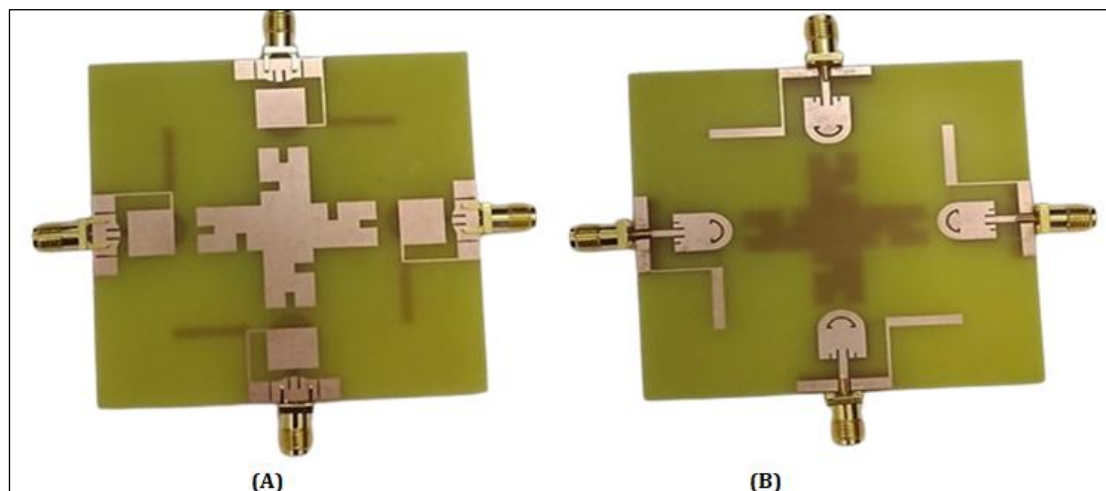
signal strength, bandwidth, and isolation, ensuring superior MIMO performance. The strategic placement of antenna elements enhances spatial diversity, reducing mutual coupling and improving overall efficiency. This design is tailored to meet the growing demands of modern wireless systems by providing stable and high-gain communication.

**Table 1:** Specifications for the Anticipated Four-Element Antenna

Parameter	L	a	c	e	g	i	r1	a1	c1	e1	g1	a2	c2	e2
Value in mm	67.9	2.3	12.5	2	10	7	4	16	3.7	8	0.5	11.45	1.5	31.9
Parameter	W	b	d	f	h	j	r2	b1	d1	f1	r3	b2	d2	f2
Value in mm	67.9	16	4.2	13	3.05	0.25	2.5	4	0.3	9	4.72	9	1.7	3

Minor inconsistencies in materials or manufacturing can cause differences between simulation and real-world performance in return loss or radiation pattern. The quality of the copper cladding and surface finish affects surface current distribution and radiofrequency losses. Fabrication flaws or incorrect surface finishing can introduce losses in the antenna design. To ensure the antenna performs as intended in simulation, we have taken great care in selecting the substrate, placing the connector, isolating components, and maintaining manufacturing tolerances. With the

given parametric values, we designed and simulated a four-element MIMO antenna using the HFSS platform. This design was then fabricated, and its radiation efficiency was tested in an anechoic chamber, followed by performance verification using the Agilent N5247A vector network analyzer (VNA). Figure 2 presents the fabricated prototype, showcasing both the front (A) and back (B) perspectives of the antenna. The testing process confirmed the antenna's performance, showing close alignment with simulation results.

**Figure 2:** Fabricated Prototype (A) Front and (B) Back Perspectives

## Results

A convergence study was conducted in HFSS by refining the mesh settings until variations in key parameters, including S-parameters, gain, and efficiency, were minimal. The simulation results remained stable beyond a specific mesh refinement threshold, confirming numerical accuracy. This ensures that the performance metrics are not influenced by meshing errors, validating the reliability of the proposed MIMO antenna design. To ensure accurate validation, the proposed four-element button mushroom MIMO antenna was tested using a vector network analyzer (VNA) and an anechoic chamber, as shown in figure 3. The anechoic chamber (Figure 3B) provides a controlled, reflection-free

environment that enables precise measurement of the antenna's radiation characteristics. A reference horn antenna was used as a receiving standard to capture radiated signals at a predefined distance, ensuring consistency in radiation performance evaluation. The antenna was mounted on a rotating platform, integrated with an automated system for azimuth and elevation adjustments, allowing for comprehensive radiation pattern analysis. The VNA setup (Figure 3A) facilitated accurate impedance matching and return loss measurements. The results obtained from the fabricated prototype were compared with the simulated data, demonstrating strong correlation and validating the antenna's effectiveness for 5G MIMO applications. The practical implementation of the proposed MIMO antenna was analyzed in

terms of mechanical robustness, usability, and safety considerations. The selected FR4 substrate ensures structural stability, making the antenna mechanically reliable for real-world applications. Additionally, the compact design enhances integration into modern 5G devices with minimal space constraints. Specific Absorption Rate (SAR)

compliance is crucial for user safety, and the antenna's low-profile structure helps in minimizing electromagnetic exposure. Future work may involve detailed SAR analysis and experimental validation to ensure regulatory compliance.

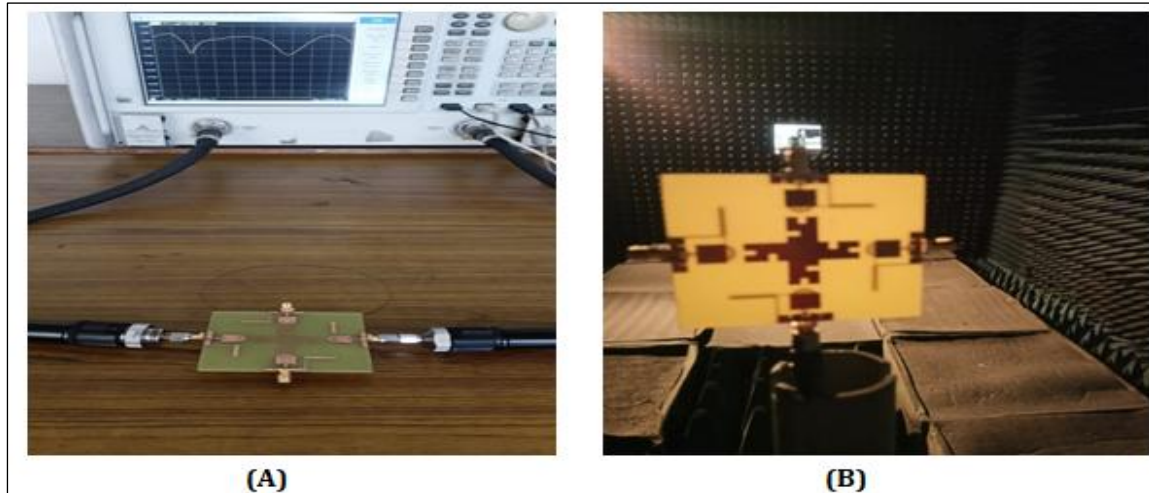


**Figure 3:** Test set-up of the Prototype with (A) VNA and in (B) Anechoic Chamber

### Reflection Coefficients and Isolation

To evaluate the impedance matching of the proposed antenna, S-parameters were analyzed using a Vector Network Analyzer (VNA), measuring S11 (return loss). A low S11 value indicates minimal signal reflection, ensuring effective impedance matching. As shown in figure 4, the simulated return loss achieves a minimum of -25.94 dB, while the measured values remain below -27.94 dB across the frequency band, confirming efficient signal transmission with minimal loss. These results validate the antenna's strong impedance matching, which is crucial for

high-performance 5G MIMO communications. Additionally, the isolation characteristics between antenna elements were analyzed, as depicted in figure 5. The simulated data indicate isolation levels consistently below -20 dB in the 3.5 to 5 GHz range, ensuring minimal interference between elements. The measured results align well, with isolation values remaining below -30 dB in the target frequency band, signifying effective signal decoupling. This high isolation minimizes mutual coupling, making the antenna ideal for 5G applications, where maintaining low interference is essential for optimal MIMO performance.

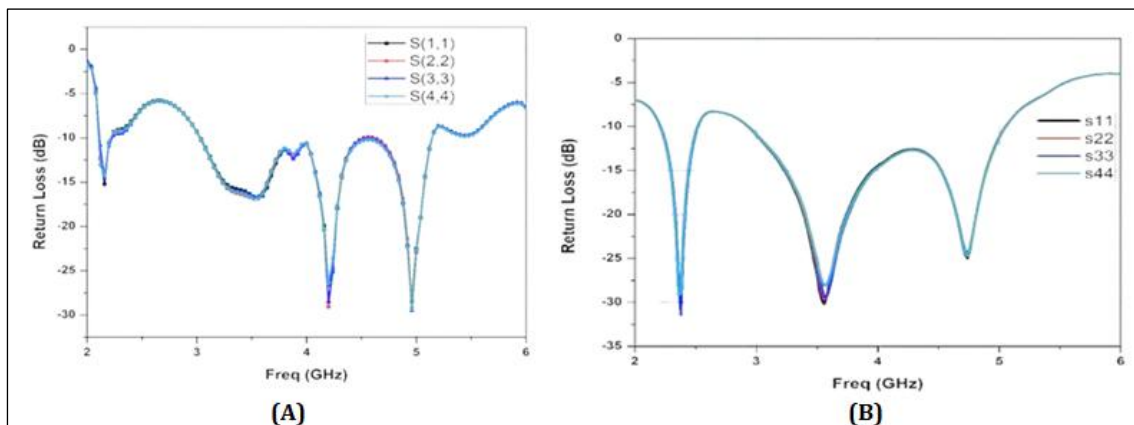


**Figure 4:** Reflection Coefficient (A) Simulated (B) Measured

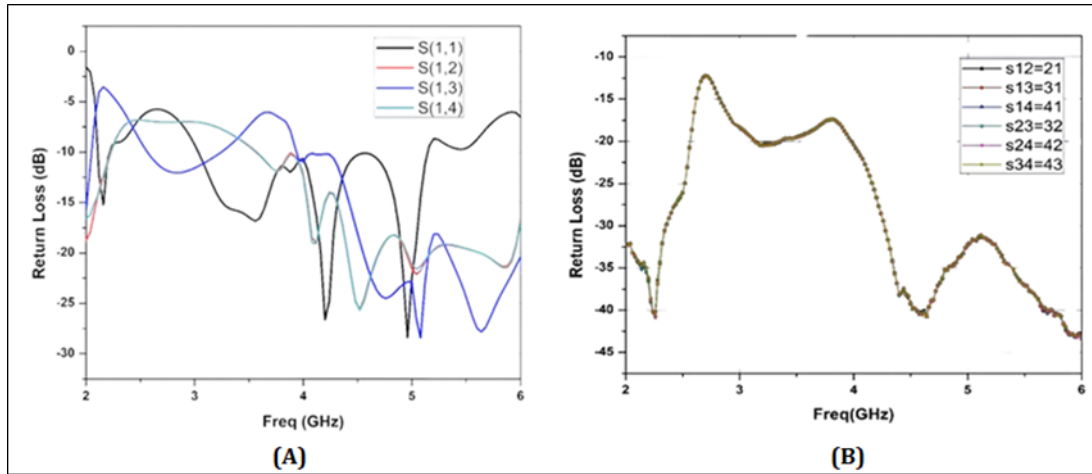


**Figure 5:** Isolation (A) Simulated (B) Measured

**Radiation Patterns**

The radiation characteristics of the antenna were analyzed at 3.5 GHz and 4.2 GHz in terms of gain and polarization. The E-plane and H-plane radiation patterns, as illustrated in figure 6 (simulated) and figure 7 (measured), exhibit stable and consistent radiation performance. The antenna demonstrates significant gain in the main lobes, reaching approximately 8–10 dB at both

frequencies, indicating efficient radiation properties suitable for 5G applications. The co-polarization patterns display well-defined directional radiation, ensuring high gain and stable performance. Meanwhile, the cross-polarization levels remain notably low, minimizing polarization impurity and reducing unwanted interference. This highlights the antenna’s effectiveness in 5G MIMO systems, ensuring reliable operation with minimal cross-polarization effects.

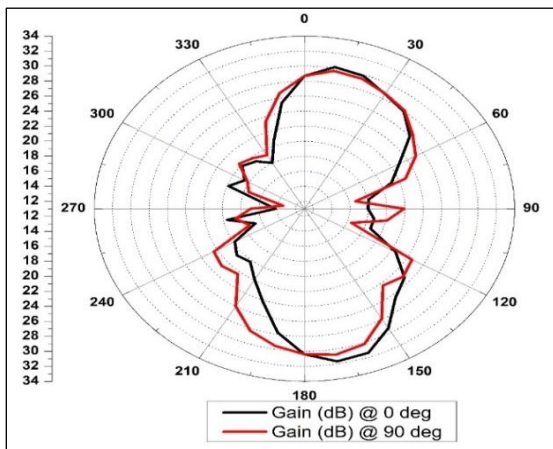


**Figure 6:** Simulated E and H Plane Patterns

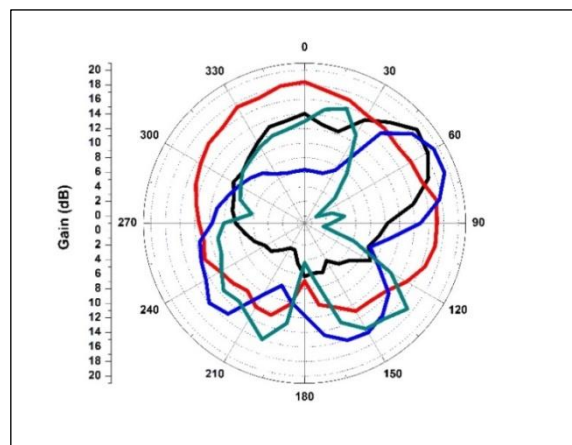


**Figure 7:** Measured E and H Plane Patterns

**Diversity Performance**

A MIMO antenna system's diversity performance is its capacity to transmit several versions of the same signal over many antennas, hence increasing signal dependability and decreasing fading. Independent propagation routes can be exploited by MIMO systems through the use of numerous spatially separated antennas. The ECC plots for the 4-element MIMO antenna show how the envelope correlation coefficient varies across a frequency range. The degree of correlation between many antennas that are close to one another is measured by the ECC. This parameter can be determined

from the S-parameters, as demonstrated in the following equation.

$$ECC = \frac{|s_{ij}^* s_{ij} + s_{ij}^* s_{jj}|^2}{(1 - |s_{ii}|^2 - |s_{jj}|^2)(1 - |s_{jj}|^2 - |s_{ii}|^2)} \dots [8]$$

According to observations, the ECC is roughly equivalent to 0.001, which is significantly less than the highest number that can be used with a MIMO antenna. These low ECC values at higher frequencies suggest good isolation and minimal correlation between the antenna components, which is beneficial for MIMO performance as it implies effective signal diversity and improved capacity. The ECC values in figure 8 remain below

0.03 across most frequency ranges, ensuring good isolation between antenna elements and optimal MIMO performance, with simulated and measured results showing strong correlation. Diversity gain is another key metric for MIMO performance, assessing how a reduction in transmitted power influences overall MIMO effectiveness. When the DG value approaches the standard threshold of 10 dB, the reduction in transmitted power has little effect on the quality of transmission. The following formula can be used to compute it.

$$DG = 10\sqrt{1 - ECC^2} \quad \dots [9]$$

The DG values in figure 9 are close to 10 dB, indicating excellent diversity performance and minimal signal degradation, further validating the antenna's effectiveness in enhancing signal reliability. Effective bandwidth is indicated by the total active reflection coefficient (TARC), which acts as an indication for the total MIMO array's return loss. It can be computed using the formula below.

$$TARC = \sqrt{\frac{(S_{11}+S_{12})^2+(S_{22}+S_{21})^2}{2}} \quad \dots [10]$$

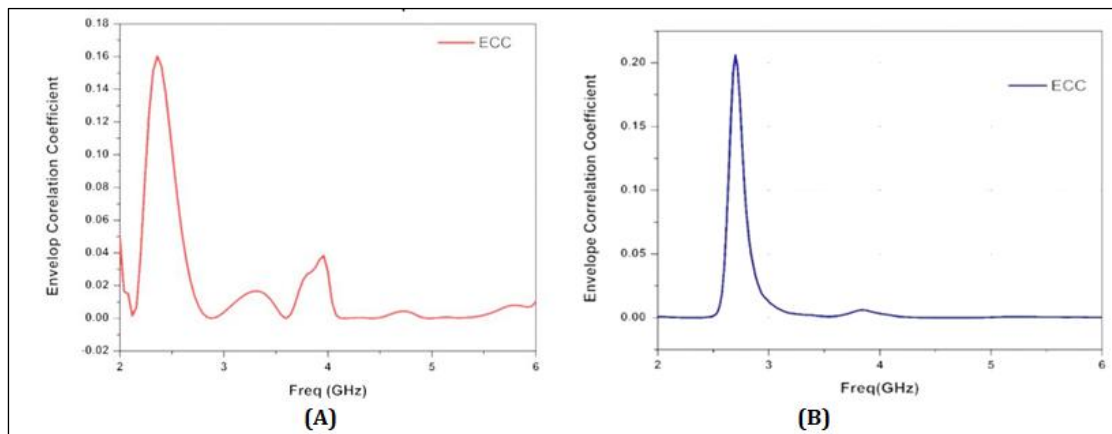


**Figure 8:** ECC (A) Simulated (B) Measured

The TARC values remain below 0.5 for most frequencies, indicating good matching and reduced reflection, which is beneficial for MIMO performance. While some discrepancies exist between the simulated and measured data, particularly in the peak values, the overall agreement between the two plots demonstrates

consistent performance, validating the antenna design's effectiveness in minimizing active reflections. In figure 10, the TARC values confirm reduced active reflection, with minimal variation between simulated and measured data, demonstrating efficient impedance matching and low reflection losses for stable 5G communication.

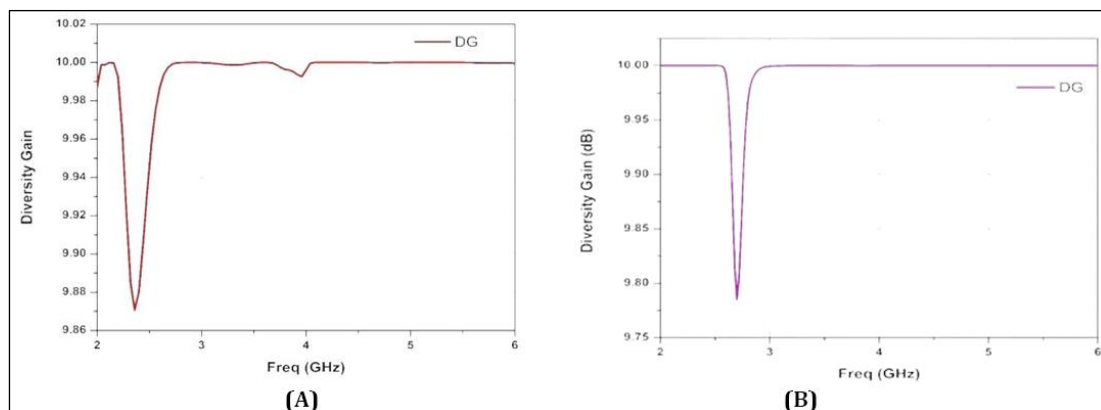


**Figure 9:** DG (A) Simulated (B) Measured

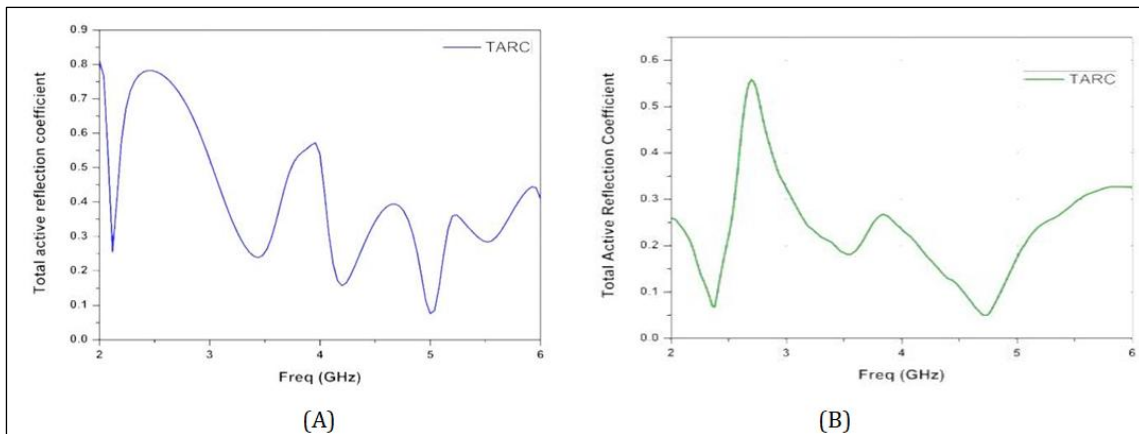


**Figure 10:** TARC (A) Simulated (B) Measured

The greatest possible transmission limit without suffering appreciable signal loss is determined by channel capacity loss. The subsequent set of formulas is used to calculate CCL.

Equations 11, 12, and 13 can be utilized to calculate CCL.

$$CCL = -\log_2 \det(a) \quad \dots [11]$$

In the above case,  $a$  is the correlation matrix.

$$a^R = \begin{pmatrix} \rho_{11} & \rho_{12} \\ \rho_{21} & \rho_{22} \end{pmatrix} \quad \dots [12]$$

$$\rho_{ii} = 1 - (|S_{ii}|^2 + |S_{ij}|^2), \text{ and} \quad \dots [13]$$

$$\rho_{ij} = -(S_{ii} * S_{ij} + S_{ij} * S_{jj}),$$

for  $i$  and  $j = 1$  and  $2$

The CCL values in figure 11 exhibit a decreasing trend as frequency increases, stabilizing around 0.5 bits/s/Hz at higher frequencies. The graph further validates this trend, indicating reduced correlation between antenna elements, which enhances system efficiency and optimizes data transmission for MIMO applications.

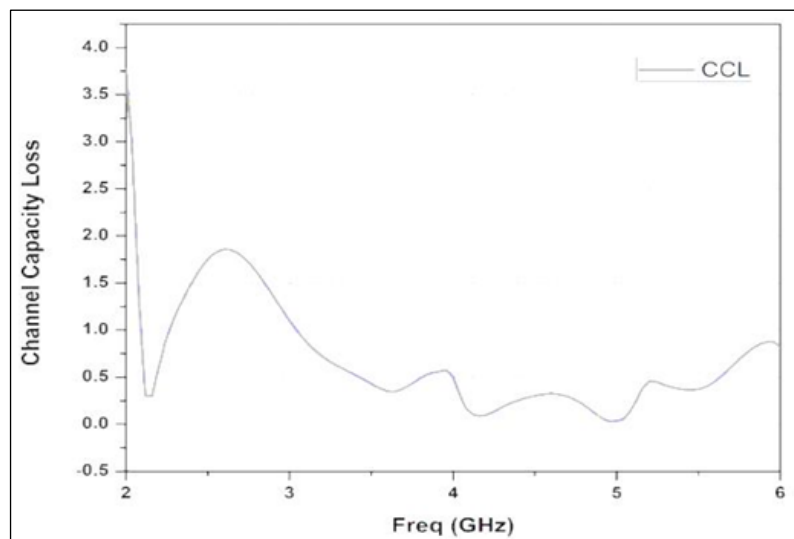


**Figure 11:** Channel Capacity Loss

Table 2 compares the measured and simulated results of the proposed antenna, demonstrating a strong correlation across key parameters. Overall, the findings demonstrate a strong correlation between the measured and simulated values, thereby validating the MIMO antenna's appropriateness for high-performance applications with favorable isolation, diversity,

gain, and impedance matching. The mean discrepancy between measured and simulated values is about 18.36%; there is variability across parameters, with a standard deviation of approximately 9.96%. The highest discrepancies were observed in TARC and gain, while impedance bandwidth had a relatively low error.

**Table 2:** A Comparison of the Measured and Simulated Results

Parameter	Impedance		TARC (dB)	DG (dB)	Isolation (dB)	Gain (dB)
	Bandwidth (GHz)	ECC				
Simulated	3.04 – 5.15	<0.01	<0.24	~9.99	-29.54	31.93
Measured	2.93 – 5.04	<0.001	<0.18	~9.99	>-27.94	23.18

## Discussion

The designed MIMO antenna resonates at two frequencies: 3.48 GHz and 4.75 GHz. Dual-band antennas enable the support of multiple technologies or communication standards within a single device by operating on two distinct frequency ranges. This makes the antenna more applicable to a variety of uses without needing several antennas for various bands. 3.48 GHz is inside the Sub-6 GHz band, which is frequently used in 5G NR (New Radio) to transport high-speed data widely. The observed isolation levels remain continuously below -20 dB throughout the frequency range, exhibiting the same trend as the result of the simulation. The measured data and

the predicted results differ slightly, but even in the worst situation, isolation stays considerably below -15 dB. Low ECC guarantees that the antenna elements can receive and send separate data, enhancing system speed and dependability. The simulated and observed values deviate slightly, but overall performance is still rather acceptable. Real-world variables, including measurement errors, environment-induced coupling, and manufacturing tolerances, can account for this discrepancy. As seen in table 3, the proposed antenna achieves the highest gain and superior isolation compared to existing designs, demonstrating its effectiveness for advanced 5G MIMO applications.

**Table 3:** Performance Comparison between the Existing and Proposed Antenna Designs

Ref. No.	No. of Ports	Size (mm)	Technique used	Isolation (dB)	Gain (dBi)	ECC	CCL (bits/s/Hz)
(21)	4	85 x 85 x 0.8	Metal strip	<-14	5.5	<0.008	-
(22)	4	58 x 60 x 1.6	Two opposite slots in the radiating elements	<-10	2.2 / 3.8	<0.08	<0.4
(23)	4	70 x 68 x 1.6	Cross-shaped structure on ground	<-18	6.4	<0.25	-
(24)	4	80 x 80 x 1.6	Z-shaped slots	<-18	5-6.8	<0.04	-
(25)	4	42 x 42	Asymptote-shaped structure	-16.4	5.1	0.02	-
(26)	4	58 x 58 x 0.7	Diagonal square with four inner lines	22	5.3	<0.01	-
This work	4	67.9 x 67.9 x 1.6	Button mushroom with DGS	<-20	23.18 dB	<0.001	<0.5

## Conclusion

This work aims to demonstrate a MIMO antenna designed for 5G applications. The system's primary board measures 67.9 x 67.9 x 1.6 mm<sup>3</sup> and it is built on an FR4 substrate. It operates over a wide frequency band, with simulated and measured results showing good impedance matching (< -10 dB), adequate isolation (-20 dB), and minimal envelope correlation (< 0.001). The high diversity gain (> 9.99) and low channel capacity loss (< 0.5) ensure efficient data transmission, while the gain levels (31.93 dB simulated, 23.18 dB measured)

are suitable for 5G requirements. Additionally, it resonates at 3.48 and 4.75 GHz with a bandwidth of 2.11 GHz, meeting the demands for 5G MIMO applications with reliable and efficient performance. Hence performance of the The proposed system exhibits high isolation and high gain along with a reduction in the overall volume of the system. These results point to a bright future for this antenna system's incorporation into the upcoming generation of smart mobile devices. To enhance adaptability across multiple 5G bands, integrating tunable components such as varactors

or MEMS switches could be explored. These elements would enable dynamic frequency tuning, allowing the antenna to operate efficiently across different sub-6 GHz bands, improving versatility for diverse 5G applications. Future work may focus on implementing and analyzing the impact of such tuning mechanisms to further optimize antenna performance.

### Abbreviations

CCL: Channel Capacity Loss, DG: Diversity Gain, DGS: Defected Ground Structure, EBG: Electromagnetic Band Gap, ECC: Envelop Correlation Coefficient, HFSS: High Frequency Structure Simulator, MIMO: Multiple-Input-Multiple-Output, SIW: Substrate Integrated Waveguide, TARC: Total Active Reflection Coefficient, VNA: Vector Network Analyzer.

### Acknowledgement

None.

### Author Contributions

All the authors have contributed to complete this work.

### Conflict of Interest

The authors declare no conflict of interest.

### Ethics Approval

Not applicable.

### Funding

This research work is not funded by any organization.

### References

- Li Q, Li G, Lee W, Lee MI, Mazzaresse D, Clerckx B, Li Z. MIMO techniques in WiMAX and LTE: a feature overview." IEEE Communications magazine. 2010 May 6; 48(5); 86-92.  
<https://doi.org/10.1109/MCOM.2010.5458368>
- Tran HH, Nguyen TT, Ta HN, Pham DP. A metasurface-based MIMO antenna with compact, wideband, and high isolation characteristics for sub-6 GHz 5G applications. IEEE Access. 2023 Jul 4;11:67737-44..
- Xi S, Cai J, Shen L, Li Q, Liu G. Dual-band MIMO antenna with enhanced isolation for 5G NR application. Micromachines. 2022 Dec 30; 14(1):95.
- Sharma P, Tiwari RN, Singh P, Kumar P, Kanaujia BK. MIMO antennas: Design approaches, techniques and applications. Sensors. 2022 Oct 14; 22(20):7813.
- Elalaouy O, El Ghzaoui M, Foshi J. Mutual coupling reduction of a two-port MIMO antenna using defected ground structure. E-Prime-Advances in Electrical Engineering, Electronics and Energy. 2024 Jun 1; 8:100557.
- Fadehan GA, Olasoji YO, Adedeji KB. Mutual coupling effect and reduction method with modified electromagnetic band gap in UWB MIMO antenna. Applied Sciences. 2022 Dec 2; 12(23):12358.
- Sandi E, Diamah A, Al Mawaddah M. High isolation MIMO antenna for 5G C-band application by using combination of dielectric resonator, electromagnetic bandgap, and defected ground structure. EURASIP Journal on Wireless Communications and Networking. 2022 Dec 27; 2022(1):125.
- Islam T, Alsaleem F, Alsunaydih FN, Alhasoon K. Mutual Coupling Reduction in Compact MIMO Antenna Operating on 28 GHz by Using Novel Decoupling Structure. Micromachines. 2023 Nov 7; 14(11):2065.
- Shakir M, Aslam S, Sarwar MU, Adnan M, Khan MR. Performance evaluation and design of 5G communication-based millimeter wave antenna. EURASIP Journal on Wireless Communications and Networking. 2021 Dec; 2021:1-0.
- Rana S, Gautam AK, Sharma S, Batra R. A Novel Compact Ultra-Wide Band MIMO Antenna for WLAN 5G & Sub-6GHz Wireless Applications. In2024 IEEE International Conference on Computing, Power and Communication Technologies (IC2PCT) 2024 Feb 9;5:1159-1164.
- Kaboutari K, Hosseini V. A compact 4-element printed planar MIMO antenna system with isolation enhancement for ISM band operation. AEU-International Journal of Electronics and Communications. 2021 May 1; 134:153687.
- Singh A, Kumar A, Kanaujia BK. High gain and enhanced isolation MIMO antenna with FSS and metasurface. Optik. 2023 Sep 1; 286:170982.
- Singh AK, Pal S. Compact self-isolated extremely low ECC folded-SIW-based slot MIMO antenna for 5G application. IEEE Antennas and Wireless Propagation Letters. 2023 Oct 2;23(1):194-8.
- Raheel K, Ahmad AW, Shah IA, Khan S, Shah SAA, Dalarsson M. Design and performance evaluation of orthogonally polarized corporate feed MIMO antenna array for next-generation communication system. IEEE Access. 2024; 12:30382-97.
- Chen S, Lu N, Sun J, Zhou C, Li C, Wu D. High-Isolation wideband MIMO antenna with offset T-Shaped slots for 5G/WLAN applications. Frontiers in Physics. 2022 Aug 19; 10:986558.
- Kiani SH, Munir ME, Savci HŞ, Rmili H, Alabdulkreem E, Elmannai H, Pau G, Alibakhshikenari M. Dual-polarized wideband 5G N77 band slotted MIMO antenna system for next-generation smartphones. IEEE Access. 2024 Feb 26; 12:34467-76.
- Girjashankar PR, Upadhyaya T. Substrate integrated waveguide fed dual band quad-elements rectangular dielectric resonator MIMO antenna for millimeter wave 5G wireless communication systems. AEU-international Journal of Electronics and Communications. 2021 Jul 1; 137:153821.
- Laxman P, Jain A. Retracted: Wideband circularly polarised antenna 'multi-input-multi-output' for wireless UWB applications. IET Wireless Sensor Systems. 2021 Dec; 11(6):259-74.
- Qin Y, Zhang L, Mao CX, Zhu H. A compact wideband antenna with suppressed mutual coupling for 5G MIMO applications. IEEE Antennas and Wireless

- Propagation Letters. 2022 Dec 15; 22(4):938-42.
20. Das GS, Chamuah BB, Beria Y, Kalita PP, Buragohain A. Compact four-element sub-6 GHz MIMO antenna for 5G applications. *Mater Today Proc.* 2023; 84:1409–14.
  21. Ding K, Gao C, Qu D, Yin Q. Compact broadband MIMO antenna with parasitic strip. *IEEE Antennas and Wireless Propagation Letters.* 2017 Jun 21; 16:2349-53.
  22. Abdulkawi WM, Malik WA, Rehman SU, Aziz A, Sheta AF, Alkanhal MA. Design of a compact dual-band MIMO antenna system with high-diversity gain performance in both frequency bands. *Micromachines.* 2021 Apr 1; 12(4):383.
  23. Kumar S, Lee GH, Kim DH, Choi HC, Kim KW. Dual circularly polarized planar four-port MIMO antenna with wide axial-ratio bandwidth. *Sensors.* 2020 Sep 30; 20(19):5610.
  24. Dwivedi AK, Sharma A, Singh AK, Singh V. Design of dual band four port circularly polarized MIMO DRA for WLAN/WiMAX applications. *Journal of Electromagnetic Waves and Applications.* 2020 Oct 12; 34(15):1990-2009.
  25. Wu A, Tao Y, Zhang P, Zhang Z, Fang Z. A compact high-isolation four-element MIMO antenna with asymptote-shaped structure. *Sensors.* 2023 Feb 23; 23(5):2484.
  26. Savcı HŞ. A four element stringray-shaped MIMO antenna system for UWB applications. *Micromachines.* 2023 Oct 18; 14(10):1944.